# Minimal modeling for passive flow control via a poro-elastic coating

Divya VENKATARAMAN[1,*], Amol MARATHE[2], Alessandro BOTTARO[1],

Rama GOVINDARAJAN[3,†]

[1] *Dipartimento di Ingegneria Civile, Chimica e Ambientale, Universitá di Genova, via Montallegro 1, 16145 Genova, Italy*

[2] *Department of Mechanical Engineering, Birla Institute of Technology and Science - Pilani, Pilani 333031, India*

[3] *Centre for Interdisciplinary Sciences, Tata Institute of Fundamental Research, 21 Brundavan Colony, Hyderabad 500075, India*

**Abstract.**

Minimal models are obtained for vortex-shedding, both from a smooth aerofoil, and from an aerofoil coated with a porous layer of flow-compliant feather-like actuators. The latter is a passive way to achieve flow control. The minimal-order model for a smooth aerofoil is extracted by analyzing the frequencies present in the flow over this aerofoil, and phenomena such as the presence of super-harmonics of these flow frequencies and existence of limit cycle behaviour for this system. Next, the minimal model for the poro-elastically coated aerofoil is realized by *linearly* coupling the minimal-order model for vortex-shedding from the smooth aerofoil with an equation for the poro-elastic coating, here modeled as a linear damped oscillator. The various coefficients in both of these models, derived using perturbation techniques, not only lead to solutions from the models that match very well with results from expensive and time-consuming computational models, but also aid in our understanding of the physics of this fluid-structure interaction problem. In particular, the minimal model for a coated aerofoil indicates the presence of distinct regimes that are dependent on the flow and coating characteristics and in this process, provide insight into the selection of optimal coating parameters, to enable flow control at low Reynolds numbers.

**Key words:** minimal model, passive flow control, poro-elastically coated aerofoil, low Reynolds number, vortex-shedding, method of multiple scales.

## 1 Introduction

An objective of this paper is to derive a minimal-order model for the vortex-shedding behind a symmetric aerofoil at an angle of attack to the free stream in a laminar flow regime. One of the motivations behind extracting such a minimal model is that it can then be coupled with any physical equation which describes the dynamics of some flow control technique, such as the use of a poro-elastic layer of flow-compliant feathers, an idea motivated from the automatic "pop-up" of *covert* feathers in birds.

*Email address for correspondence: vdivya8@yahoo.co.in. Presently at the International Centre for Theoretical Sciences, Tata Institute of Fundamental Research, Bangalore (India).

† *On lien* from the Jawaharlal Nehru Centre for Advanced Scientific Research, Bangalore (India).

The derivation of a low-order model for vortex-shedding behind an aerofoil without such a flow-control coating, (henceforth referred to as "smooth"), is thus a crucial preliminary step in characterizing the structural and physical parameters of this coating, in order to obtain the desired modifications in the aerofoil's aerodynamic performance. The first part of this paper addresses the case of the smooth aerofoil, while the second part considers the *passive* flow-control technique of using a poro-elastic coating of compliant actuators over this aerofoil.
In the first part of this paper, in order to extract a reduced-order model for the phenomenon of vortex-shedding behind an aerofoil, its characteristics are analysed - deriving motivation from earlier studies performed for vortex-shedding from cylinders. Some signature of these characteristics is in fact contained in a quantity obtained by globally integrating over the computational domain (Akhtar *et al.* (2009)) - such as the lift and drag for this aerofoil. Here, a reduced-order model will be derived for the non-dimensional lift coefficient. Further, this model is of the smallest possible order that can accurately capture the dynamics of the lift coefficient, and thus, henceforth such a model will be called a minimal-order model, or more simply, minimal model. Once this minimal model is known, the various parameters in it for a specific case (parametrized here by the angle of attack), are appropriately determined, so that results from this model match well with the computational results for the same case.

In the second part of the paper, a minimal model for a poro-elastically coated aerofoil is realized by *linearly* coupling the minimal model for the vortex-shedding behind a smooth aerofoil with an equation of a linear damped oscillator, here taken to describe the dynamics of the porous, compliant coating. The basic motivation for developing and studying a minimal model in this manner is that although numerical as well as experimental parametric studies for this flow control technique have shown its effectiveness in applications such as drag reduction and delay in stall angles in the recent past (including but not limited to Bakhtian *et al.* (2007), Favier *et al.* (2009), Venkataraman & Bottaro (2012), Brücker & Weidner (2013)), a theoretical model can help in better understanding the underlying physics of this coupled fluid-structure interaction problem, without the need for performing time-consuming computations and/or experiments and extensive parameter search to determine "optimal" control parameters. This paper is in fact a first step towards rigorously and theoretically characterising *passive* flow-control/actuator parameters which should as well as should not be used, to obtain favourable modifications in the flow field.
This paper begins, in§2, with an overview of facts in non-linear dynamics used to develop the low-order model for the smooth aerofoil, followed by a highlight of the characteristics of the aerofoil's lift coefficient in this context. §3 outlines the development of the minimal model for the *smooth* aerofoil while §4 derives its analytical solution and in this process, determines the model parameters, so that results from this model match with those from the computational model. From §5 onwards, the second part of the paper begins which describes the minimal model for a *coated* aerofoil, starting with a derivation of the closed-form expression for the solution of such a coupled system (analogous to how this was achieved for the case of a *smooth* aerofoil). §6 presents an overview of computations performed to arrive at the minimal model. §7 compares the results from the computational model with those from the minimal model, hence proving its effectiveness, while §8 summarises the paper and lists some perspectives for future work.

## 2 Limit cycles and vortex-shedding

### 2.1 Characteristics of limit cycles

When the present system of vortex-shedding from an aerofoil is compared with generic non-linear dynamical systems exhibiting limit cycles, the following facts are seen to be pertinent towards extracting the low-order model:
(i) The equation for the low-order model should be *autonomous* (i.e., the coefficients of various derivative terms do not depend explicitly on time). It is important to note here that only those autonomous equations with negative linear damping (which allows small perturbations to grow) and *at least one counter-acting* positive non-linear damping term (which will push large perturbations back to the equilibrium state), are capable of producing limit cycles.
(ii) Once the flow parameters, such as the Reynolds number and, as in the present case, the shape of the aerofoil and its angle of attack are fixed, the long time history of the vortex-shedding from the body is periodic in the Reynolds number range of our consideration (cf. figure 1(a)), and independent of initial conditions. Such a system is said to be a *self-excited oscillator*.

### 2.2 Characteristics of vortex-shedding from aerofoil

In order to derive the minimal model for vortex-shedding behind an aerofoil, the NACA0012 aerofoil is taken to be at an angle of attack of 10°; the chord-based Reynolds number is taken to be 1100. Details of the numerical approach and results are provided in Venkataraman (2013). To develop a low-order model, the characteristics of the lift coefficient for this configuration (obtained from the computational model), in time and frequency domains, as shown in Figure 1, are considered.

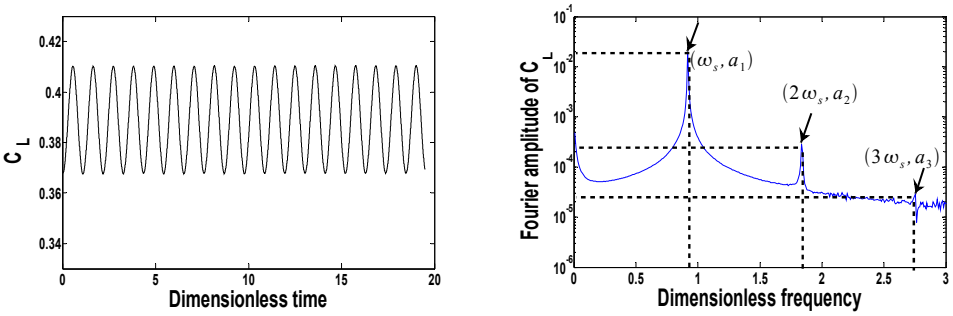


Figure 1: (Left): Time evolution of lift coefficient for an aerofoil at an incidence of 10° to the incoming flow at $Re = 1100$; (right) Fourier spectrum of lift coefficient. Simulations from Venkataraman & Bottaro (2012).

It can be seen from Figure 1(b) that after a peak at the fundamental frequency $\omega_s$ (which is in fact the frequency of vortex-shedding), there is a peak with substantial amplitude at $2\omega_s$ (followed by a smaller peak at $3\omega_s$). To account for such super-harmonics of flow frequencies, a non-linear model consisting of at least one quadratic non-linearity must be considered (Venkataraman (2013)).
However, an equation consisting of non-linearities of order at most two, and no

higher-order non-linearities (such as cubic or higher), does not model a self-excited oscillator, since for each new initial condition, the dynamics settles down to a new closed orbit (hence showing the non-existence of a limit cycle).

# 3 Development of a minimal model

## 3.1 Condition for existence of limit cycles

Considering that a third-order non-linearity is required in the model equation for producing a limit cycle, a generic constant coefficient non-linear ordinary differential equation, with all possible quadratic and cubic non-linearities, is taken:

$$\frac{d^2x}{dt^2}+x = c\frac{dx}{dt}+\alpha_1 x^2+\alpha_2 x\frac{dx}{dt}+\alpha_3(\frac{dx}{dt})^2+\beta_1 x^3+\beta_2 x^2\frac{dx}{dt}+\beta_3 x(\frac{dx}{dt})^2+\beta_4(\frac{dx}{dt})^3 \quad (3.1)$$

where $c$ is the coefficient of linear damping, $\alpha_i$ for $i = 1, 2, 3$, and $\beta_j$ for $j = 1, 2, 3, 4$ are the coefficients of quadratic and cubic non-linear damping terms, respectively. For this system, a *necessary* (but not *sufficient*) condition for the existence of a limit cycle is given below. This condition is obtained by using Lindstedt's perturbation method, the detailed derivation for which is present in Venkataraman (2013). This necessary condition for the existence of a limit cycle imposes certain restrictions on these coefficients, by means of deriving the following expression for the amplitude $A$ of the limit cycle:

$$A = 2\sqrt{\frac{-\mu}{\alpha_2(\alpha_1+\alpha_3)+\beta_2+3\beta_4}}; \quad (3.2)$$

(where $\mu$ is the second-order approximation to the linear damping coefficient $c$, having the same sign as $c$), and observing that a limit cycle for this system will exist *only if* the expression (3.2) for the amplitude $A$ is real. Thus, if the linear damping coefficient $c$ (or equivalently its second-order approximation $\mu$) is *positive* (so that system (3.1) has negative linear damping), the quantity $\alpha_2(\alpha_1+\alpha_3)+\beta_2+3\beta_4$ must be *negative* to ensure the existence of a limit cycle.

## 3.2 Application to the case of vortex-shedding

Since the characteristics for aerofoil vortex shedding are dependent only on the flow Reynolds number and the aerofoil's angle of attack, and not on the initial conditions, this system can be expected to exhibit a stable limit cycle. Based on the analysis in the previous paragraph, it is possible to deduce which non-linear terms must be present in the generic system (3.1) to yield limit cycles.

To simplify our analysis of how the non-linearities of different orders interact with each other, and in order to develop a minimal-order model that accurately captures the dynamics of vortex-shedding, only one of the terms of quadratic and cubic non-linearities will be taken to be non-zero. From equation (3.2), it can be seen that the coefficients $\beta_1$ and $\beta_3$ (corresponding to the non-linear terms $x^3$ and $x\dot{x}^2$) do not play any role for the amplitude $A$ to be real. Hence, the two non-linear terms $x^3$ and $x\dot{x}^2$ will be taken to be absent. The dependence of the existence of limit cycle on the coefficients $\alpha_1$, $\alpha_2$, $\alpha_3$, $\beta_2$ and $\beta_4$ is summarised in table 1 (with the linear

| **Case** | $\alpha_1$ | $\alpha_2$ | $\alpha_3$ | $\beta_2$ | $\beta_4$ | **Existence of limit cycle** |
|---|---|---|---|---|---|---|
| 1 | 1 | 0 | 0 | -1 | 0 | No |
| 2 | 1 | 0 | 0 | 0 | -1 | No |
| 3 | 0 | 1 | 0 | -1 | 0 | Yes |
| 4 | 0 | 1 | 0 | 0 | -1 | Limit cycle exists only for initial conditions with $\dot{x}$ negative or zero. |
| 5 | 0 | 0 | 1 | -1 | 0 | No |
| 6 | 0 | 0 | 1 | 0 | -1 | Yes |

Table 1: Dependence of limit cycle existence on the non-linearities in equation (4.1).

damping coefficient $c$ fixed to 1).
From this table, it can be seen that only cases 3 and 6 yield limit cycles. Further, from a comparative analysis of the phase portraits (i.e plots of $\dot{x}$ versus $x$) for these two cases (Venkataraman (2013)), it can be seen that the convergence to a limit cycle is slightly faster in case 6, in which the non-linearities involved are $\dot{x}^2$ and $\dot{x}^3$. Our physical system is one where the limit cycle is attained fairly quickly, i.e. within a few oscillation time scales. Hence the equation taken to model the system under consideration is:

$$\frac{d^2x}{dt^2} + x = \frac{dx}{dt} + (\frac{dx}{dt})^2 - (\frac{dx}{dt})^3 \tag{3.3}$$

It must be noted here that the coefficients of various terms in this equation need not all have a magnitude of unity in general. These coefficients are selected appropriately as detailed below, for the system under consideration.

# 4 Model parameters using the method of multiple scales

Denoting the variable being modeled as $C_L$ (the non-dimensional lift coefficient), the model equation with all its unknown parameters can be written as:

$$(\frac{d^2}{dt^2} + \omega^2)C_L = \mu\frac{d}{dt}C_L - \alpha(\frac{d}{dt}C_L)^3 + \beta(\frac{d}{dt}C_L)^2 + \omega^2\widetilde{C_L} \tag{4.1}$$

where the parameters $\mu$, $\alpha$ and $\beta$ are all positive. The presence of an extra constant $\omega^2\widetilde{C_L}$ here accounts for the fact that the mean lift coefficient $\widetilde{C_L}$ for an aerofoil is non-zero.
To determine the parameters $\omega^2$, $\mu$, $\alpha$ and $\beta$, the analytical form of the solution for equation (4.1) is determined, which in turn is dependent on these parameters. Once the closed-form solution is known, it is matched with the simulation results (for instance, such as those shown in figure 1) to determine these model parameters.

Equation (4.1) will be solved by the method of multiple scales (Strogatz (1994), Venkataraman (2013)). We consider the problem when the damping and nonlinearities are weak; that is, we take $\mu$, $\alpha$ and $\beta$ to be of $O(\delta)$, where $\delta << 1$ is a

bookkeeping parameter and in fact, measures how *strongly* non-linear the system is. Thus in physical terms, $\delta$ translates to a parameter that measures the ratio between the Fourier amplitudes corresponding to the fundamental frequency and its second super-harmonic, $a_1$ and $a_2$ respectively (cf. Figure 1(b)).
The method of multiple scales is used to determine a second-order approximate solution in $\delta$ for the lift coefficient $C_L(t)$ by introducing the fast, slow and slower time scales given by $T_0 = t$, $T_1 = \delta t$, and $T_2 = \delta^2 t$. By following this procedure and imposing an additional physical constraint that the amplitude of the oscillations of $C_L(t)$ has attained saturation with a non-zero value, the following analytical form is obtained for $C_L(t)$:

$$C_L(t) = a_0 + a_1 \cos(\omega_s t) + a_2 \cos(2\omega_s t) + a_3 \sin(3\omega_s t) \tag{4.2}$$

where $a_0$, $a_1$, $a_2$, $a_3$ and $\omega_s$ are parameters of the limit cycle obtained for this case (Venkataraman (2013)). These parameters can be determined in terms of the parameters of the *minimal* model $\omega$, $\mu$, $\alpha$ and $\beta$, when the latter are known. Conversely, the parameters of the *minimal* model can be determined in terms of $a_0$, $a_1$, $a_2$, $a_3$ and $\omega_s$, when the exact form and characteristics of the limit cycle are known (such as, from results of *computational* models, as in the present case).

# 5 Linear minimal model for *coupled* fluid-structure interaction: derivation of solution

To follow the simplest approach, we consider the reduced-order model for the feathery coating as a linear spring, described by a linear damped oscillator's equation. In the spirit of developing a *minimal* model for this coupled fluid-structure interaction problem, the dynamics of the coating, expressed by the variable $\theta$, is interpreted as the displacement of the fluid-coating interface from an equilibrium position, as shown in figure 2. Thus in this context, it must be noted that the structure model equation governs only the *overall* displacement of the coating *as a whole*, and not the dynamics of the angular displacements of the invidual feathers. Hence, interaction effects can be neglected in the *overall* structure model, thus explaining the *minimality* of this model. When such a linear damped oscillator's equation is coupled with the minimal model for vortex-shedding behind a smooth aerofoil derived earlier, the coupled system is given by:

$$\ddot{C_L} + \omega^2 C_L - \omega^2 \widetilde{C_L} - \mu \dot{C_L} + \alpha(\dot{C_L})^3 - \beta(\dot{C_L})^2 = \rho_1 \theta \tag{5.1}$$

$$\ddot{\theta} + c\dot{\theta} + \omega_1^2 \theta = \rho_2 (C_L - \widetilde{C_L}) \tag{5.2}$$

where $\rho_1$ and $\rho_2$ are constants enforcing a linear coupling between the fluid and structure systems (and $\widetilde{C_L}$ was defined earlier in §4).
As done in §4, this coupled system can also be solved by the method of multiple scales, to find the general form of the solution, $C_L$ and $\theta$, in terms of the model parameters. Conversely, given the form of the solution (for instance from the computational data, as in the present case), it is possible to find the model parameters in terms of the numerical/physical characteristics of the computations. In addition, it is also possible to make inferences about "optimal" structure model parameters that yield the desired behaviour for the solution of the coupled system.

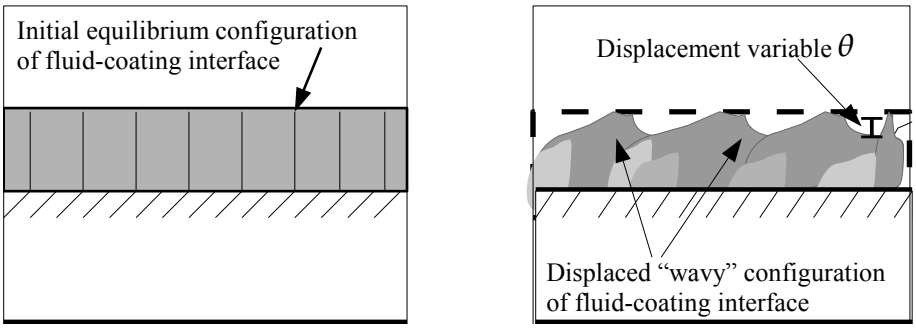


Figure 2: Fluid-coating interface : (left) - initial undisturbed configuration (i.e., without any forcing from the fluid) - the vertical lines here denote a discrete number of feathers spread uniformly in this layer; (right) - disturbed configuration showing the displacement variable $\theta$. Note here that the colour gradient in this disturbed layer characterizes the non-uniform, time-varying porosity (i.e., darker shades denote clustering of feathers while lighter shades stand for areas with a lower instantaneous concentration of feathers).

As outlined in §4, we consider the coupled problem when the damping and nonlinearities for the fluid component, the damping/dissipation for the structure component as well as the coupling between the fluid and structure parts are weak. Thus, by taking $\mu$, $\alpha$, $\beta$, $c$, $\rho_1$ and $\rho_2$ all to be of $O(\delta)$ (where $\delta$ is a bookkeeping parameter measuring how strong the non-linearity in the system is, $\delta << 1$), we determine a second-order approximate solution in $\delta$ for the lift coefficient and the fluid-coating interface. The fact that all the fluid as well as structure damping terms and fluid-structure coupling terms are of $O(\delta)$ physically means that all these damping and coupling effects are *weak* compared to the oscillation effects of the two *stand-alone* fluid and structure components of this coupled fluid-structure system.
Equations (5.1) and (5.2) are solved, analogous to the case of the smooth aerofoil, by introducing the fast, slow and slower time scales, given by $T_0 = t$, $T_1 = \delta t$, and $T_2 = \delta^2 t$, respectively, and separating coefficients of like powers of $\delta$ (Venkataraman *et al.* (2013)). The solutions involve arbitrary functions $A_1(T_1, T_2)$ and $A_2(T_1, T_2)$, in terms of the time scales $T_1$ and $T_2$ (but constant with respect to the time scale $T_0$), and to ensure bounded solutions (by eliminating secular terms), four solvability conditions are obtained (involving $\dfrac{\partial A_1}{\partial T_1}$, $\dfrac{\partial A_1}{\partial T_2}$, $\dfrac{\partial A_2}{\partial T_1}$ and $\dfrac{\partial A_2}{\partial T_2}$). Finally using the polar transformations $A_1(t) = \dfrac{1}{2}a_1(t)e^{\iota\gamma_1(t)}$ and $A_2(t) = \dfrac{1}{2}a_2(t)e^{\iota\gamma_2(t)}$ in the expressions for $C_L(t)$ and $\theta(t)$ respectively, closed-form solutions for the *modified* lift coefficient and coating interface are obtained. Combining the solvability conditions corresponding to $A_1$ with the polar transformation above for $A_1$, the following modulation equations arise:

$$\dot{a_1}(t) = \frac{\delta}{2}\left\{\frac{\mu}{2}a_1(t) - \frac{3}{8}\alpha\omega^2 a_1^3(t)\right\}, \tag{5.3}$$

$$\dot{\gamma_1}(t) = -\delta^2\left\{\frac{\mu^2}{8\omega} + \frac{3}{16}\mu\alpha\omega a_1^2(t) - \frac{\beta^2}{6}\omega a_1^2(t) - \frac{27}{256}\alpha^2\omega^3 a_1^4(t) - \frac{\rho_1\rho_2}{2\omega(\omega-\omega_1)(\omega+\omega_1)}\right\}; \tag{5.4}$$

and likewise for $A_2$:

$$\dot{a_2}(t) = -\frac{\delta}{2}ca_2(t)\ , \tag{5.5}$$

$$\dot{\gamma_2}(t) = -\delta^2 \left\{ \frac{\iota c^2}{8\omega_1} + \frac{\rho_1 \rho_2}{2\omega_1(\omega - \omega_1)(\omega + \omega_1)} \right\}. \tag{5.6}$$

Again under the initial assumption that $C_L(t)$ and $\theta(t)$ both have reached their equilibrium states, equations (5.3) and (5.5) can be solved. This results in two possible values of $a_1$: 0 and $\frac{2}{\omega}\sqrt{\frac{\mu}{3\alpha}}$ (exactly as in the calculations for the case of smooth aerofoil). Further, the only possibilities for steady-state condition for $a_2(t)$ are $c = 0$ or $a_2(t) = 0$. The trivial solution of *both* $a_1(t) = 0$ and $a_2(t) = 0$ can be ruled out. The qualitative characteristics of the solutions for the other three cases are summarized in Table 2 (with further details in Venkataraman *et al.* (2013)). It must be noted here that $\omega_{s,1} = \omega - \frac{(\delta\mu)^2}{16\omega} - \frac{2(\delta\beta)^2\mu}{9\alpha\omega} - \frac{(\delta\rho_1)(\delta\rho_2)}{2\omega(\omega - \omega_1)(\omega + \omega_1)}$ and $\omega_{s,2} = \omega_1 - \frac{(\delta\rho_1)(\delta\rho_2)}{2\omega_1(\omega - \omega_1)(\omega + \omega_1)}$.

| **Case** | **Steady-state amplitudes of fluid and structure,** $a_1$ **and** $a_2$ | **Physical interpretation of steady-state conditions** | **Features of fluid and structure steady-state solutions,** $C_L(t)$ **and** $\theta(t)$ |
|---|---|---|---|
| 1 : Weak structure-to-fluid coupling | $a_1 = \sqrt{\frac{4\mu}{3\alpha\omega^2}}$ ; $a_2 = 0$. | Dissipation constant $c$ of the coating arbitrarily large (i.e., energy dissipation by the coating very large). | (a) Form of $C_L(t)$ similar to that for *smooth* aerofoil, given in equation (4.2), with frequency distribution exhibiting *a unique* frequency $\omega_{s,1}$ and its super-harmonics; (b) No super-harmonics of $\omega_{s,1}$ in spectrum of $\theta(t)$. |
| 2 : Weak fluid-to-structure coupling | $a_1 = 0$ ; $a_2$ arbitrarily large constant. | Dissipation constant $c$ is 0 (i.e., no energy dissipation by the coating due to oscillations). | (a) Dynamics of coupled system dictated by structure; (b) *Only one* frequency $\omega_{s,2}$ (*without* any super-harmonics) in spectrum of both $C_L(t)$ and $\theta(t)$. |
| 3 : Two-way coupling | $a_1 = \sqrt{\frac{4\mu}{3\alpha\omega^2}}$; $a_2$ arbitrarily large constant. | Dissipation constant $c = 0$ (as for case 2). | (a) Dynamics of coupled system combination of cases 1 and 2 (i.e., frequency spectra of both $C_L(t)$ and $\theta(t)$ exhibit frequencies $\omega_{s,1}$ and $\omega_{s,2}$) ; (b) Super-harmonics of *only* $\omega_{s,1}$ seen, *only* in spectrum of $C_L(t)$. |

Table 2: Cases of steady-state solutions dependent on coating parameters.

In all of the above three cases, we can have the possibilities of at least one of $\omega_{s,1}$ or $\omega_{s,2}$ being zero. It is important to note that if $\omega_{s,1}$ is zero, then so is $\omega_{s,2}$ and vice-versa, which by an order of magnitude analysis, is seen to be possible only if $\omega \sim \omega_1$

(Venkataraman *et al.* (2013)), which is nothing but the *resonant* condition for the coupled fluid-structure system. The other possibility is the *non-resonant* condition, where both $\omega_{s,1}$ and $\omega_{s,2}$ are non-zero. A summary of the effects produced on the characteristics of the lift coefficient (in the form of change in mean lift or change in lift fluctuations about this mean), is presented in Table 3.

| **Case** | **Resonant frequency conditions** | **Non-resonant frequency conditions** |
|---|---|---|
| 1 : Weak structure-to-fluid coupling | $\sqrt{\frac{4\mu}{3\alpha\omega^2}}$ dominates mean lift increase | Changes in coating parameters do not *directly* affect lift characteristics |
| 2 : Weak fluid-to-structure coupling | Mean lift *increase* by $O(\delta)$ when: (a) **structure-fluid coupling** parameter $\rho_1$ **increased**; (b) **compliance increased** so that steady-state amplitude $C_0$ of oscillations of the coating interface is large. | Lift fluctuations *decrease* if $\frac{\delta\rho_1 C_0}{(\omega-\omega_1)(\omega+\omega_1)} < \sqrt{\frac{4\mu}{3\alpha\omega^2}}$ |
| 3 : Two-way coupling | Same as case 2 | Lift fluctuations *increase avoided* if $\frac{\delta\rho_1 C_0}{(\omega-\omega_1)(\omega+\omega_1)} < \sqrt{\frac{4\mu}{3\alpha\omega^2}}$ |

Table 3: Effect of change in coating parameters on characteristics of lift coefficient.

## 6 Results from computational model: brief overview

In order to relate the theoretical results obtained in §2 and §3 to the results from the computational model for the symmetric aerofoil, the flow configuration is initially taken to be simpler. For this, the flow over a flat plate, with rounded leading and trailing edges, first aligned with the free-stream, and then oriented at an angle of incidence to it, is considered. As the next step, this tilted flat plate "morphs" into a symmetric aerofoil, and the flow dynamics over this aerofoil is related with the results for the simpler configuration (i.e., flat plate) as well as the theoretical results in earlier sections. In this way, such computations provide a good prototype flow for us to understand the mechanisms of lift enhancement or drag reduction. Details of all these results are present in Venkataraman *et al.* (2013).

For the case of an aerofoil, various simulations were performed for a poro-elastically coated aerofoil at 10° angle of incidence to the free-stream, with different structural as well as physical parameters (such as the rigidity frequency, the length of reference feathers, the placement of the coating on the aerofoil, etc. - cf. Venkataraman & Bottaro (2012)). It was observed that in none of these cases, the dynamics of either the fluid or the structure systems (as captured by the quantities $C_L(t)$ and $\theta(t)$) exhibited only one frequency *without* any super-harmonics (i.e., the characteristics of case 2). Further, from the perspective of the dynamics of the fluid component, the Fourier spectrum either showed one frequency *with* its super-harmonics, or two

unrelated frequencies along with super-harmonics for *only one* of these (i.e., cases 1 and 3, respectively).
Hence, for the derivation of the model parameters in terms of the characteristics of the simulation results (analogous to how this was done for the case of smooth aerofoil), an illustrative case that corresponds with case 1 of §5 is selected. In this case, the first half of the suction side of the aerofoil is poro-elastically coated. The angular rigidity frequency $\omega_r$ (which is also taken to be the dominant structure frequency) is set to the value 2.8972, which is half of the fundamental frequency in the fluid system $\omega_f$ (which in turn is the frequency of vortex-shedding - cf. Venkataraman (2013), Venkataraman *et al.* (2013)). The position of the reference control elements on the aerofoil is shown in figure 3. Some aspects of the results from the computations for this case will be presented in §7, in the context of extracting parameters of the minimal model, the results for which yield a good match with those from computational model.

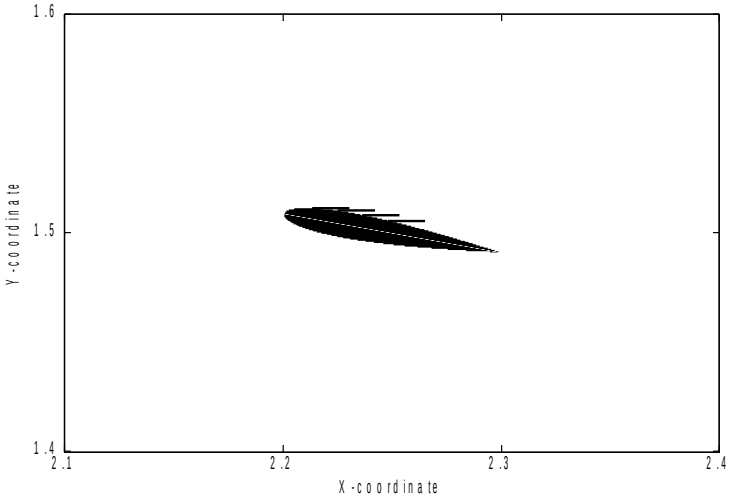


Figure 3: Placement of the poro-elastic layer on the aerofoil, depicted by the position of four reference feathers (shown here by the thick, black lines near the leading edge of the aerofoil).

# 7 Comparison with simulation results

## 7.1 Case of smooth aerofoil

From Figure 1(b) which shows the Fourier spectrum of the lift coefficient, one gets the following values for the fundamental frequency $\omega_s$, amplitudes corresponding to the fundamental frequency $a_1$, twice the fundamental frequency $a_2$, and three times the fundamental frequency $a_3$:

$$\omega_s = 2\pi \times 0.9222 = 5.7944 \; ; \quad a_1 = 0.02119 \; ; \quad a_2 = 3.46 \times 10^{-4} \; ; \quad a_3 = 1.9 \times 10^{-5}. \tag{7.1}$$

With these *input* values, we get the following values of the model parameters for equation (4.1):

$$\omega = 5.8039 \; ; \; \delta\mu = 0.1249 \; ; \; \delta\alpha = 11.0102 \; ; \; \delta\beta = 4.6234. \tag{7.2}$$

Again substituting these parameters in the model equation (4.1) and by numerically solving it, we can compare this solution with the computational results, as done in Figure 5(a).

### 7.2 Case of poro-elastically coated aerofoil

This section highlights some aspects of the computational results for a poro-elastically coated aerofoil shown in figure 3, and with coating parameters as explained in §6.

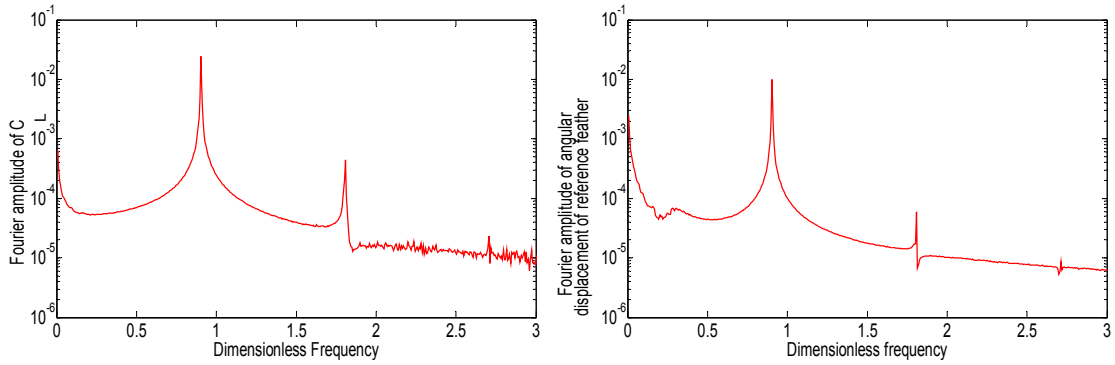


Figure 4: (Left) Fourier spectrum for the time signal of the lift coefficient for aerofoil at 10° angle of attack, with poro-elastic coating where the rigidity frequency $\omega_r$ is set equal to half the frequency of vortex-shedding; (right) Fourier spectrum for the time evolution of the angular displacement of the reference feather nearest to the trailing edge. This figure shows the case where the poro-elastic layer spans 50% of the suction side.

The left frame of figure 4 shows the Fourier decomposition for the time evolution of the lift coefficient for this aerofoil, while the right frame shows the Fourier decomposition for the time signal of the angular displacement of a reference feather closest to the trailing edge. In these, a sharp peak at a certain *unique* frequency is observed, followed by peaks with amplitude of smaller magnitudes at twice and three times these frequencies. Hence, this case corresponds to case 1 (i.e., when the coating interface has *zero* steady-state amplitude for its displacement, and the lift has a *non-zero* steady-state amplitude), with the fluid and structure systems both oscillating at the same frequency $\omega_{s,1}$.
From the left and right frames of figure 4, one gets the following values for the fundamental frequency $\omega_{s,1}$, amplitudes of the lift coefficient corresponding to the fundamental frequency and its second and third super-harmonics $l_1$, $l_2$ and $l_3$ respectively; and amplitude of the angular displacement of the reference feather (closest to the trailing edge) $\phi_1^{'}$ corresponding to the fundamental frequency:

$$\omega_{s,1} = 2\pi \times 0.9039 = 5.6794 \ ; \ l_1 = 0.0245 \ ; \ l_2 = 4.459 \times 10^{-4} \ ; \ l_3 = 8.123 \times 10^{-6} \ ; \ \phi_1^{'} = 0.01003. \tag{7.3}$$

From this value of $\phi_1^{'}$ and the known value of the length of the feather, one can evaluate the vertical displacement of the coating interface $\theta_1^{'} = 8.551 \times 10^{-7}$. With these *input* values, we get the following values of the parameters for equations (5.1)

and (5.2):

$$\omega = 5.6907 \ ; \ \delta\mu = 0.0453 \ ; \ \delta\alpha = 3.106 \ ; \ \delta\beta = 4.4571 \ ; \ \omega_1 = 0 \ ; \ \delta\rho_1 = 0 \ ; \ \delta\rho_2 = -1.13 \times 10^{-3}. \tag{7.4}$$

It must be recalled that for this case, the dissipation constant $c$ of the reference feather is allowed to be arbitrary, and hence can be taken to be arbitrarily large. This is in line with the physical consideration that the steady-state amplitude $a_2$ of the *stand-alone* structure part of the coupled system is zero.
Thus, substituting the values obtained in equation (7.4) and by numerically solving it, we can compare this solution with the simulation results, as done in figure 5(b).

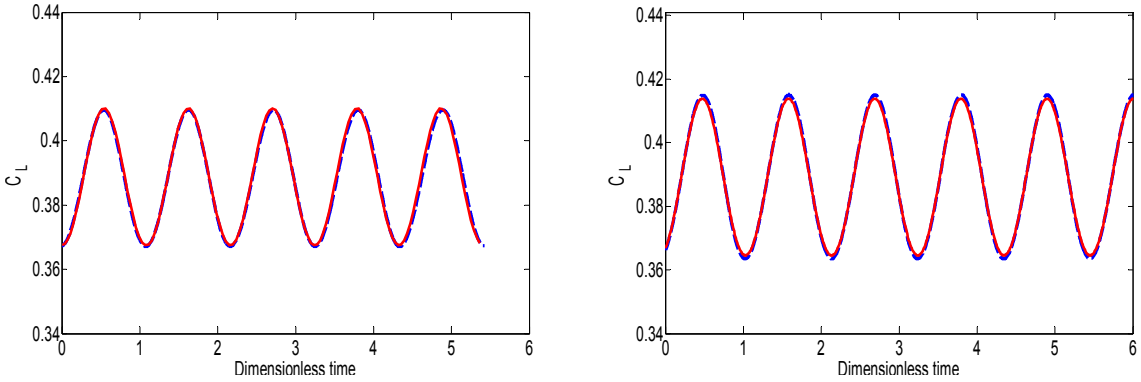


Figure 5: Comparison of model and simulation results of lift coefficient for: (left) smooth aerofoil and; (right) aerofoil with the poro-elastic coating shown in figure 4. The dashed curve (blue online) shows the results from the computational model while the solid curve (red online) shows results from the minimal models.

It can be seen that the results from the computational model and those from the minimal model agree very well with each other, for both smooth as well as poro-elastically coated aerofoils. It can also be easily verified that the steady-state solutions are independent of the initial conditions (Venkataraman (2013)). All of these results indicate the effectiveness of the minimal models for vortex-shedding, behind smooth as well as coated aerofoils.

## 8 Conclusions

In the first part of this paper, a minimal model for vortex-shedding behind an aerofoil at an angle of incidence to the free-stream has been developed. For this, the characteristics of the lift coefficient of the aerofoil (which is an integral quantity that contains the signature of the characteristics of vortex-shedding) are analysed. The Fourier spectrum of the lift coefficient for this configuration reveals amplitude peaks at a fundamental frequency (equal to the frequency of vortex-shedding), and its second and third superharmonics, in decreasing order of amplitudes. To account for such dynamical features, a non-linear model with exactly one quadratic and one cubic non-linearity is developed, by analyzing which non-linear models with quadratic and cubic non-linearities have trajectories converging to (unique) limit

cycles, independent of initial conditions. For this non-linear model, suitable model parameters are determined (by deriving the analytical solution using the method of multiple scales, and then comparing it with the computational results), which yields a good match between the solutions obtained from the minimal model and computations.
In the second part of this paper, a minimal model for the lift coefficient of the aerofoil considered before, but now with a poro-elastic coating on a part of its suction side, has been developed. For this, the minimal-order model for a smooth aerofoil has been linearly coupled with a linear damped oscillator for the dynamics of the poro-elastic layer. For this coupled non-linear model, a closed-form expression for its limit cycle is derived in terms of generic (unknown) fluid, structure and coupling parameters (similar to the analysis done for the case of smooth aerofoil). In the course of this analysis, three physical cases could be segregated, based on the possibilities of whether the steady-state amplitudes of the stand-alone *fluid oscillator* and the stand-alone *structure oscillator* was zero or not. The closed-form expressions for all these cases yielded conditions on resonant and non-resonant regimes of fluid and structure frequencies, thus giving an insight into possible selection of structure and coupling parameters that are capable of rendering, for instance, reduced lift fluctuations as compared to the case of the smooth aerofoil.
Several simulation results for coated aerofoils, with different extents and placements of coating over the suction side, conducted in the course of this study, are seen to fall in one of the two cases from the above possibilities. From this, the fluid, structure and coupling parameters, that yield matching of trajectories obtained from the minimal model and computations, are determined (analogous to how this was done for the case of smooth aerofoil). All of the above observations indicated the effectiveness of the minimal model for smooth as well as coated aerofoils.
Possible extensions of this work can be to formulate progressively non-linear models for the structure and coupling parts, to be able to trust the effectiveness of such a poro-elastic coating, for more complex configurations as well as for different flow regimes.

## Acknowledgements

The first author would like to thank Dr. Jan Pralits and Prof. Giovanna Vittori at the University of Genova, Italy for useful discussions for the first part of this work. Also, financial support received from the Jawaharlal Nehru Centre for Advanced Scientific Research, Bangalore, India and the Centre for Interdisciplinary Sciences, Tata Institute of Fundamental Research, Hyderabad, India is gratefully acknowledged, where the first author conducted a part of this work as a Visiting doctoral student.

## References

1. S.H. Strogatz, *Nonlinear dynamics and chaos* (Addison-Wesley, Reading, MA, 1994).
2. D. Venkataraman and A. Bottaro,"Numerical modeling of flow control on a symmetric aerofoil via a porous, compliant coating," Phys. Fluids **24**, 093601 (2012).
3. N.M. Bakhtian, H. Babinsky, A.L.R. Thomas and G.K. Taylor,"The low Reynolds number aerodynamics of leading edge flaps,"in *Proceedings of the 45th AIAA Aerospace Sciences Meeting and Exhibit, January 8-11, 2007, Reno, NV* (AIAA, Reston, VA, 2007), pp. 8018-8030.

4. C. Brücker and C. Weidner, "Separation control via self-adaptive hairy flaplet arrays," in *Proceedings of the ERCOFTAC International Symposium on Unsteady Separation in Fluid-Structure interaction, June 17-21, 2013, Mykonos, Greece.*
5. J. Favier, A. Dauptain, D. Basso, and A. Bottaro,"Passive separation control using a self-adaptive hairy coating,"J. Fluid Mech. **627**, 451 (2009).
6. I. Akhtar, O.A. Marzouk, and A.H. Nayfeh, "A van der Pol-Duffing oscillator model of hydrodynamic forces on canonical structures, "ASME J. Comput. Nonlinear Dyn. **4**, 041006 (2009).
7. D. Venkataraman,"Flow control using a porous, compliant coating of feather-like actuators," Ph.D thesis (Department of Civil, Chemical and Environmental Engineering, University of Genova, Italy) 2013; available at $http://www.dicca.unige.it/bottaro/Presentation\%20group/Thesis\_DivyaVenkataraman.pdf$.
8. D. Venkataraman, A. Bottaro and R. Govindarajan, "A minimal model for flow control on an aerofoil using a poro-elastic coating," J. Fluids Struct. **47**, pp. 150-164 (2014).